The Plant Journal (2007) doi: 10.1111/j.1365-313X.2006.02985.x

A lysine-rich arabinogalactan protein in Arabidopsis is essential for plant growth and development, including cell division and expansion

Jie Yang[1,2,3], Harjinder S. Sardar[1,2,3], Kathleen R. McGovern[2], Yizhu Zhang[1,2,3] and Allan M. Showalter[1,2,3]*

[1]*Department of Environmental and Plant Biology,*

[2]*Department of Biological Sciences, and*

[3]*Molecular and Cellular Biology Program, Ohio University, Athens, OH 45701-2979, USA*

Received 26 July 2006; revised 28 September 2006; accepted 4 October 2006.
*For correspondence (fax +1 740 593 1130; e-mail showalte@ohio.edu).

Summary

Arabinogalactan proteins (AGPs), a family of hydroxyproline-rich glycoproteins, occur throughout the plant kingdom. The lysine-rich classical AGP subfamily in Arabidopsis consists of three members, AtAGP17, 18 and 19. In this study, AtAGP19 was examined in terms of its gene expression pattern and function. *AtAGP19* mRNA was abundant in stems, with moderate levels in flowers and roots and low levels in leaves. *AtAGP19* promoter-controlled GUS activity was high in the vasculature of leaves, roots, stems and flowers, as well as styles and siliques. A null T-DNA knockout mutant of *AtAGP19* was obtained and compared to wild-type (WT) plants. The *atagp19* mutant had: (i) smaller, rounder and flatter rosette leaves, (ii) lighter-green leaves containing less chlorophyll, (iii) delayed growth, (iv) shorter hypocotyls and inflorescence stems, and (v) fewer siliques and less seed production. Several abnormalities in cell size, number, shape and packing were also observed in the mutant. Complementation of this pleiotropic mutant with the WT *AtAGP19* gene restored the WT phenotypes and confirmed that AtAGP19 functions in various aspects of plant growth and development, including cell division and expansion, leaf development and reproduction.

Keywords: Arabidopsis, arabinogalactan protein, cell division, cell expansion, glycosylphosphatidylinositol anchor, plant growth and development.

Introduction

Arabinogalactan proteins (AGPs) are hyperglycosylated members of the hydroxyproline-rich glycoprotein superfamily, and decorate the surfaces of cells throughout the plant kingdom. The protein backbones of AGPs are rich in Pro/Hyp (hydroxyproline), Ser, Ala and Thr, and are modified by the addition of type II arabinogalactan polysaccharides and arabinose oligosaccharides (Gaspar *et al.*, 2001; Showalter, 2001). AGPs react specifically with β-glucosyl Yariv reagent (Yariv *et al.*, 1962, 1967), a chemical reagent used to precipitate AGPs as well as to probe their function.

AGPs are divided into several classes: classical AGPs, lysine-rich classical AGPs, AGP peptides, fasciclin-like AGPs (FLAs), and other chimeric AGPs. Classical AGPs are 85–151 amino acids in length and consist of an N-terminal signal peptide, a Pro/Hyp-rich AGP central domain and a C-terminal glycosylphosphatidylinositol (GPI) lipid anchor addition sequence (Schultz *et al.*, 1998; Showalter, 2001). Upon GPI anchor cleavage by phospholipases, AGPs are released from the plasma membrane to the extracellular matrix. Lysine-rich AGPs are a subclass of the classical AGPs and have a small lysine-rich region within the classical AGP domain. The lysine-rich region is not glycosylated, which has allowed the production of peptide-specific antibodies (Gao and Showalter, 2000; Gao *et al.*, 1999; Zhang *et al.*, 2003). AGP peptides are distinguished by small AGP domains, which are typically 10–15 amino acids in length; these AGP domains are flanked by a signal peptide and in many cases by a GPI anchor addition sequence. FLAs contain both AGP and fasciclin-like domains (Schultz *et al.*, 2002). In Arabidopsis, there are 14 classical AGPs, three lysine-rich AGPs, 12 AG peptides and 21 FLAs (Schultz *et al.*, 2002).

In addition to FLAs, other chimeric AGPs exist (Borner *et al.*, 2003; Schultz *et al.*, 2002). Xylogens in *Zinnia elegans* and Arabidopsis contain both an AGP domain and a non-specific lipid transfer protein domain (Motose *et al.*, 2004). In rice, two chimeric AGPs, an early nodulin-like protein and a lipid transfer-like protein, were recently identified (Mashiguchi *et al.*, 2004).

While the structure and composition of AGPs are well characterized from biochemical and molecular biology studies (Gaspar *et al.*, 2001; Kieliszewski and Shpak, 2000; Sun *et al.*, 2004b, 2005; Zhao *et al.*, 2002), their biological roles have remained elusive and are only now beginning to be understood. AGPs are implicated as functioning in many cellular and physiological processes (Majewska-Sawka and Nothnagel, 2000; Showalter, 2001), including somatic embryogenesis (van Hengel *et al.*, 2002), cell proliferation (Langan and Nothnagel, 1997; Serpe and Nothnagel, 1994), cell expansion (Willats and Knox, 1996), xylem differentiation and development (Gao and Showalter, 2000; Motose *et al.*, 2001; Zhang *et al.*, 2003), programmed cell death (Gao and Showalter, 1999), pollen tube growth (Wu *et al.*, 2000) and plant hormone actions (Suzuki *et al.*, 2002).

AGP mutants represent a new, powerful and direct means to assign function to individual AGPs. RNA interference (RNAi) of *AGP1* in moss (*Physcomitrella patens*) resulted in reduced cell length (Lee *et al.*, 2005). When both Arabidopsis xylogen genes (*AtXYP1* and *AtXYP2*) are knocked out, the mutant leaves have discontinuous veins (Motose *et al.*, 2004). A mutation in *AtFLA4* results in irregular cell expansion, thinner cell walls and increased sensitivity to salt (Shi *et al.*, 2003). AtAGP30, a non-classical AGP containing six cysteines in the C-terminus, enhances the response to abscisic acid (ABA), and is required for root regeneration and seed germination (van Hengel and Roberts, 2003). In addition to AtAGP30, two lysine-rich AGPs, CsAGP1 from cucumber (*Cucumis sativus*) and LeAGP1 from tomato (*Lycopersicon esculentum*), also respond to phytohormones. *CsAGP1* is responsive to gibberellin and implicated in stem elongation (Park *et al.*, 2003). *LeAGP1* is up-regulated by cytokinin, and its over-expression results in tomato plants that phenotypically resemble cytokinin-over-expressing plants (Sun *et al.*, 2004a).

The three lysine-rich AGPs in Arabidopsis, AtAGP17, AtAGP18 and AtAGP19, are likewise important for plant growth and development. One incomplete knockout mutant of *AtAGP17*, designated as *rat1* (resistance to *Agrobacterium*), is deficient in binding of *Agrobacterium* to its roots (Gaspar *et al.*, 2004; Nam *et al.*, 1999). AtAGP18 is essential for female gametogenesis, as functional megaspores in *AtAGP18* RNAi mutants failed to enlarge and divide, resulting in ovule abortion and reduced seed set (Acosta-Garcia and Vielle-Calzada, 2004). In order to complement our previous work with a tomato lysine-rich AGP, namely LeAGP1 (Gao and Showalter, 2000; Gao *et al.*, 1999; Li and Showalter, 1996; Sun *et al.*, 2004a,b, 2005), and further our understanding of the lysine-rich AGPs in Arabidopsis, AtAGP19 was examined here in terms of its genetic expression and function in Arabidopsis growth and development, based upon mutant analysis and genetic complementation.

Results

AtAGP19 *is classified as a lysine-rich AGP*

The *AtAGP19* gene (At1g68725) is 833 bp in length, and the predicted size of its mRNA is 744 nucleotides. While the consensus intron splicing site for most genes contains the sequence GT…AG, *AtAGP19* has a single intron with a non-consensus intron splicing site of GT…AT. Seven lysine-rich AGPs from various plant species have been identified to date: LeAGP1 (Gao *et al.*, 1999; Li and Showalter, 1996) in tomato, NaAGP4 in *Nicotiana alata* (Gilson *et al.*, 2001), AtAGP17, 18 and 19 in Arabidopsis (Schultz *et al.*, 2002), CsAGP1 in cucumber (Park *et al.*, 2003) and PtaAGP6 in pine (*Pinus taeda*) (Zhang *et al.*, 2003). All have an N-terminal signal sequence, a central AGP domain containing a small lysine-rich region, and a C-terminal GPI anchor addition sequence (Figure 1). While LeAGP1 and NaAGP4 share 80% amino acid sequence identity, other lysine-rich AGPs have lower amino acid sequence similarities and identities. For example, AtAGP17 and AtAGP18 are 64% and 54% similar and identical to each other, respectively. On the other hand, AtAGP19 has only 38% and 28% amino acid sequence similarity and identity to AtAGP17, and 45% and 34% similarity and identity to AtAGP18. Attention was focused on *AtAGP19*, as a mutation in this gene has the potential to provide a more dramatic phenotype and would be less likely to experience compensation by the two other subfamily members.

AtAGP19 *expression is tissue-specific and developmentally controlled*

Northern blot analyses of Arabidopsis seedlings and mature organs using gene-specific probes revealed that expression of *AtAGP17*, *18* and *19* in Arabidopsis was organ-specific (Figure 2a). The *AtAGP17* transcript was found in seedlings, rosette leaves, flowers and stems, but not roots. *AtAGP19* transcript levels were high in stems, moderate in roots and flowers, low in seedlings, and barely detectable in mature rosette leaves. Similarly, *AtAGP18* was expressed in roots,

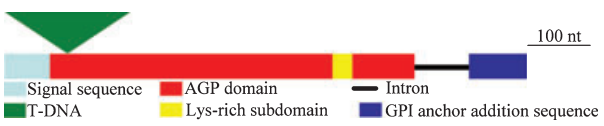

Figure 1. Gene structure of *AtAGP19*.
A T-DNA insertion in *AtAGP19* (in SALK_038728) is shown and not drawn to scale.

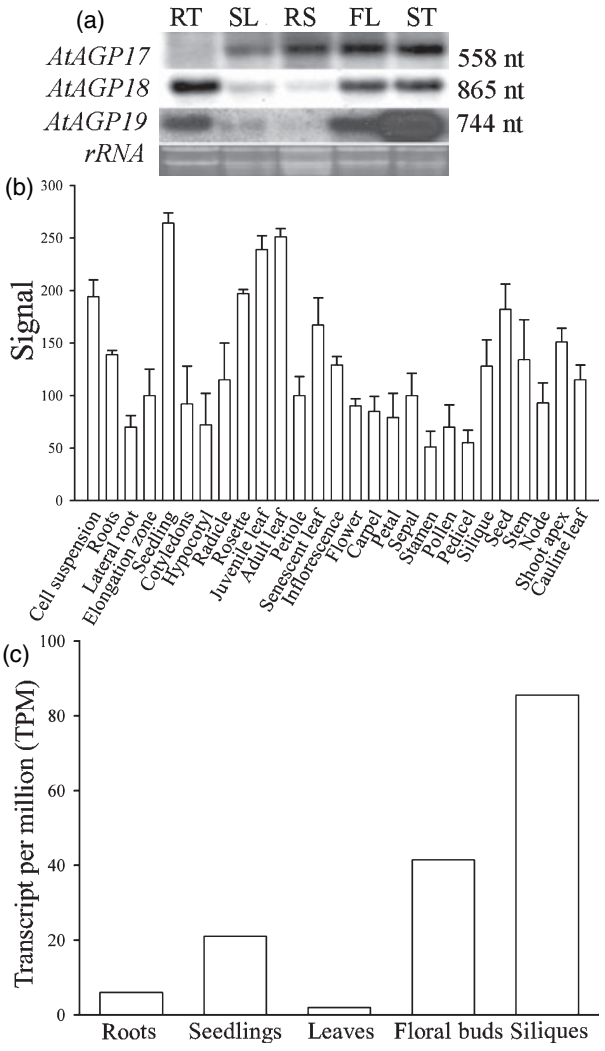

Figure 2. Genetic expression of *AtAGP19*.
(a) Transcript abundance of *AtAGP17*, *18* and *19* determined by Northern blotting. Aerial parts of 10-day-old seedlings (SL) and 4-week-old roots (RT), rosettes (RS), flowers (FL) and stems (ST) were examined. rRNAs were stained with ethidium bromide to show equal loading. The sizes of *AtAGP17*, *18*, and *19* mRNA are shown on the right.
(b) Expression pattern of *AtAGP19* by microarray analyses. Values are means + SD.
(c) Expression of *AtAGP19* detected by massively parallel signature sequencing. Roots and leaves were 21 days old, seedlings were 3 days old, and floral buds and developing siliques were harvested from 5-week-old plants.

flowers and stems and weakly expressed in seedlings and rosettes.

To investigate the expression of *AtAGP19* at the tissue level, expression of the GUS gene under the control of the *AtAGP19* promoter was examined in transgenic Arabidopsis plants (Figure 3). GUS staining was consistently found in the vasculature of leaves, roots, stems and flowers (pedicels, sepals, petals and filaments). Both light- and dark-grown 3-day-old seedlings expressed GUS in the cotyledons, hypocotyls and roots, but not in root hairs or root tips. In 7-day-old-seedlings, the root staining pattern resembled that of the 3-day-old seedlings, although the staining in hypocotyls was stronger and broader, with the apical portion of the hypocotyl being more heavily stained than the basal portion. In rosette leaves, the vascular tissues in the blade and petiole were stained, with pronounced staining at the hydathodes, epidermal structures specialized for water secretion. Staining in new leaves was strong throughout, but decreased and became restricted to the vasculature as the leaves matured. Old or senescent leaves showed little or no staining, consistent with the Northern blot analysis of mature leaves. Staining in cauline leaves was similar to that in rosette leaves. GUS activity was also found in leaf and stem trichomes. Young stems were stained throughout their lengths, while older stems showed greatest staining in the apical portion (data not shown). Anthers lacked GUS staining, while the style, ovary walls and transmitting tract were stained. Siliques also demonstrated GUS staining. These results indicate that *AtAGP19* expression is developmentally controlled, with young organs being preferentially stained, and organ- and tissue-specific, with the vasculature, style and developing siliques displaying the greatest amount of GUS staining.

In addition to Northern blotting and GUS analyses, *AtAGP17*, *18* and *19* expression was also examined by accessing publicly available microarray data online (Zimmermann *et al.*, 2004). Microarray data indicated that *AtAGP18* was the most abundantly expressed lysine-rich AGP, followed by *AtAGP17* and *19*. The relative transcription levels of these three AGPs were corroborated by Northern blotting, RT-PCR and GUS staining (data not shown). Furthermore, our expression patterns of *AtAGP17*, *18* and *19* were largely consistent with the microarray data. Low to moderate levels of *AtAGP19* transcription were detected in wild-type (WT) Arabidopsis plants and cell cultures, and Figure 2(b) shows the mean signal intensities for *AtAGP19* in a pool of microarray experiments. When Arabidopsis seedlings of WT and various mutant backgrounds were treated with biotic and abiotic stresses (such as wounding, heat, hormones and hormone inhibitors, pathogen-derived elicitors), *AtAGP19* mRNA levels did not change significantly (data not shown). Microarray data confirmed the widespread expression of *AtAGP19*, although there were some minor differences with regard to relative expression levels between the *AtAGP18* and *AtAGP19* microarray profiles and our results. Two reasons may account for such differences. First, the Arabidopsis plants used in microarray experiments were grown by different laboratories and might not be harvested at identical stages. Second, the detection sensitivity of microarray experiments is limited by RNA quantities (Meyers *et al.*, 2004), and *AtAGP19* transcript abundance is relatively low.

Another approach to analyze gene expression is by MPSS (massively parallel signature sequencing), which is more sensitive and accurate in quantifying gene expression at low

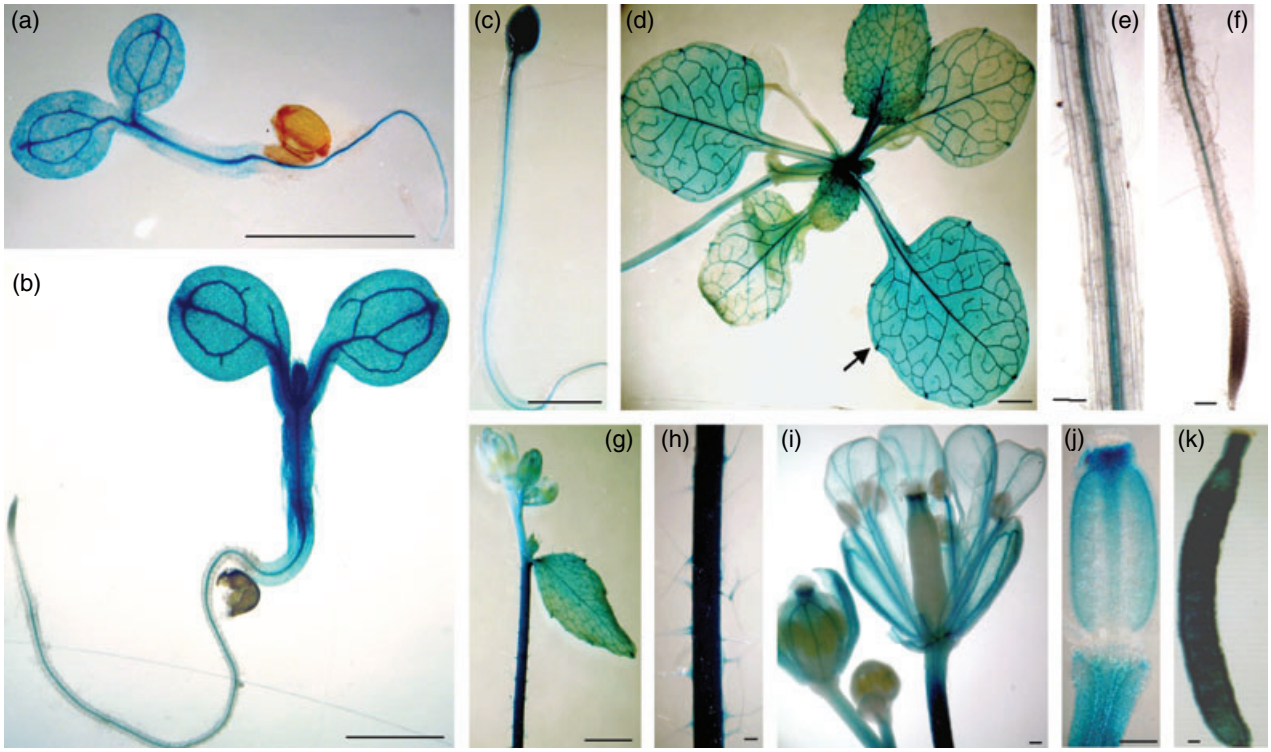

Figure 3. GUS staining in transgenic plants harboring the $P_{AtAGP19}$:GUS reporter gene construct.
(a,b) Light-grown 3- and 7-day-old seedlings, respectively. (c) Dark-grown 3-day-old seedling. (d) Rosette. Staining was restricted to the vasculature in mature leaves. The arrow indicates a hydathode. (e,f) Root and root tip. (g) Inflorescence including a cauline leaf. (h) Magnified view of the stem in (g). (i) Open flower. (j) Carpel in an unopened flower. Note staining of the style, ovary wall and transmitting tract. (k) Silique. Bars = 1 mm for (a)–(d) and (g), and 0.1 mm for (e), (f) and (h)–(k).

levels compared to microarray experiments (Meyers *et al.*, 2004). MPSS analysis of Arabidopsis revealed that *AtAGP19* was most highly expressed in elongating siliques and immature floral buds. *AtAGP19* transcripts were also found in germinating seedlings, and the abundance was low in roots and leaves (Figure 2c). Consistent with microarray data, MPSS showed that overall *AtAGP19* mRNA levels were low.

Identification and genetic complementation of a null knock-out mutant of AtAGP19

A reverse genetics approach was taken to determine the function of AtAGP19. Only one null T-DNA mutant line of *AtAGP19* (SALK_038728) has been identified (Alonso *et al.*, 2003) and was obtained from the Arabidopsis Biological Resource Center (ABRC). The location of the T-DNA insertion was verified by sequencing (Figure 1). RT-PCR demonstrated that *AtAGP19* mRNA was absent in the homozygous *atagp19* mutant (Figure 4a).

Although the heterozygous mutant was not phenotypically different from WT, the *atagp19* homozygous mutant displayed considerable abnormal phenotypes with respect to various aspects of plant growth and development. Complementation of the mutant with the WT *AtAGP19* gene under the control of its own promoter restored *AtAGP19*

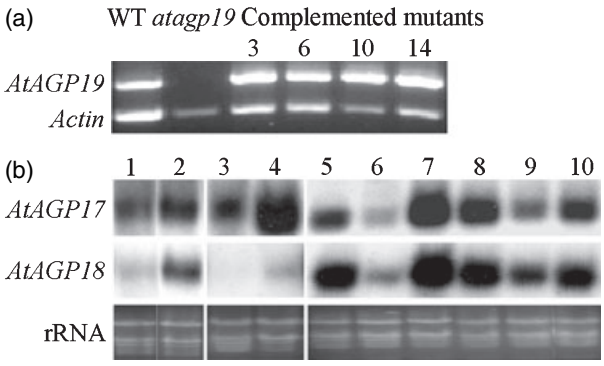

Figure 4. Expression of *AtAGP17*, *18* and *19* in the *atagp19* mutant and complemented mutant plants.
(a) RT-PCR of total stem RNA showed that *AtAGP19* mRNA was absent in the *atagp19* mutant but present in complemented plants. Actin was used as the internal control.
(b) Northern blotting of *AtAGP17* and *18* in the *atagp19* mutant. Lane 1, wild-type (WT) seedling; lane 2, *atagp19* mutant seedling; lane 3, WT rosette; lane 4, *atagp19* mutant rosette; lane 5, WT stem; lane 6, *atagp19* mutant stem; lanes 7–10, stem RNA of complemented *atagp19* mutant lines 3, 6, 10 and 14. rRNAs were stained with ethidium bromide to show equal loading.

mRNA (Figure 4a) as well as the WT phenotypes. This confirmed that the mutant phenotypes were caused by the knockout of *AtAGP19*. SALK lines of *AtAGP17* (SALK_101062) and *AtAGP18* (SALK_117268) were also

examined, but neither showed any readily identifiable phenotypes compared with those observed in *atagp19*.

As there are three lysine-rich AGPs in Arabidopsis, it was important to know whether the two homologs of *AtAGP19*, namely *AtAGP17* and *18*, were compensating for *AtAGP19* in the *atagp19* null mutant. As shown in Figure 4(b), both *AtAGP17* and *18* transcription was down-regulated in the mutant stem. In complemented mutants, *AtAGP17* and *18* expression returned to normal levels. In *atagp19* seedlings, while *AtAGP18* transcription was elevated, the *AtAGP17* mRNA level showed little change. In contrast, in mutant rosettes, *AtAGP18* expression did not change, while the *AtAGP17* mRNA level increased.

Beyond these molecular phenotypes, several remarkable phenotypes were readily apparent in the *atagp19* mutant. These phenotypes were analyzed in detail and reported below.

Reduced hypocotyl cell length in the atagp19 *mutant*

atagp19 hypocotyls were 75% of the length of WT hypocotyls when grown under long-day conditions, which corresponded to a reduction in hypocotyl cell length but not cell number. However, hypocotyl length was not compromised when *atagp19* seedlings were grown in the dark. These results indicate that AtAGP19 function is regulated by light. Moreover, although cell length was reduced in the light-grown mutant, hypocotyl diameter, cell width and cell layers were all similar to those of WT (Table 1).

The atagp19 *mutant grows more slowly and has altered leaf morphology and pigmentation*

During vegetative growth, *atagp19* had fewer rosette leaves compared to WT plants at the same age. Moreover, *atagp19* rosette leaves were smaller and more round and had shorter petioles than WT (Figure 5a,b).

atagp19 mutants, including leaves, stems and sepals, were lighter green than WT plants throughout the life cycle. Pigment content analyses demonstrated that *atagp19* rosette leaves contained less chlorophyll and anthocyanin compared to WT (Figure 5c,d). Microscopic analysis showed that there was no significant difference in chloroplast numbers in mesophyll cells between the mutant and WT (data not shown).

Table 1 Hypocotyl parameters of wild type (WT) and *atagp19* mutant seedlings

Conditions	Parameters	WT	*atagp19*
Light	Hypocotyl length (mm)	2.8 ± 0.1	2.1 ± 0.1
	Hypocotyl cell number	18.1 ± 0.8	19.8 ± 0.6
	Average epidermal cell length (μm)	155.9 ± 6.4	110.3 ± 8.4
	Hypocotyl diameter (μm)	330.8 ± 14.2	320.5 ± 6.7
	Average epidermal cell width (μm)	13.2 ± 0.7	13.4 ± 0.6
Dark	Hypocotyl length (mm)	16.2 ± 0.5	16.5 ± 1.3

Values are expressed as mean ±95% CI.

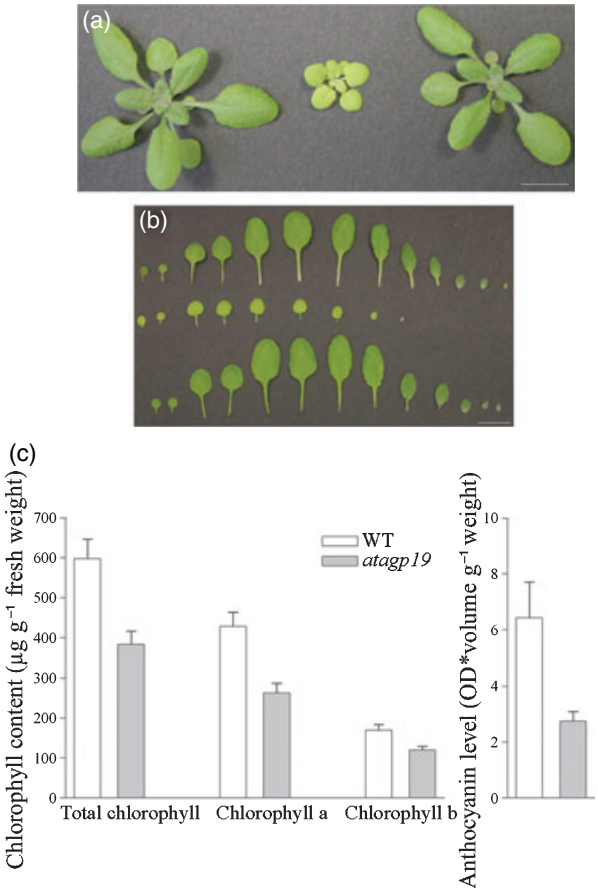

Figure 5. Morphology and pigmentation differences between wild-type (WT) and *atagp19* mutant leaves.
(a) Three-week-old rosettes of WT (left), *atagp19* mutant (center) and complemented plants (right). Bar = 1 cm.
(b) Rosette leaves of WT (top), *atagp19* mutant (center) and complemented plants (bottom). Bar = 1 cm.
(c) The *atagp19* mutant had lower chlorophyll and anthocyanin levels than WT. Error bars indicate SE ($n = 5$).

In order to explore causes of the smaller leaf size, the abaxial epidermis of the first two true leaves of WT and *atagp19* was studied. Both the size and number of the epidermal cells were found to be decreased in the mutant. However, stomata cells appeared normal in terms of morphology and fraction of total epidermal cells (Figure 6).

As plants matured, WT rosette leaves curled down and *atagp19* mutant leaves remained flat (Figure 7a). To determine the causes of flat mutant leaves, a differential interference contrast (DIC) microscope was used to visualize mesophyll cells. Palisade mesophyll cells were smaller in the mutant than in WT (Figure 7b,c), whereas spongy mesophyll cells in the *atagp19* mutant were more regular

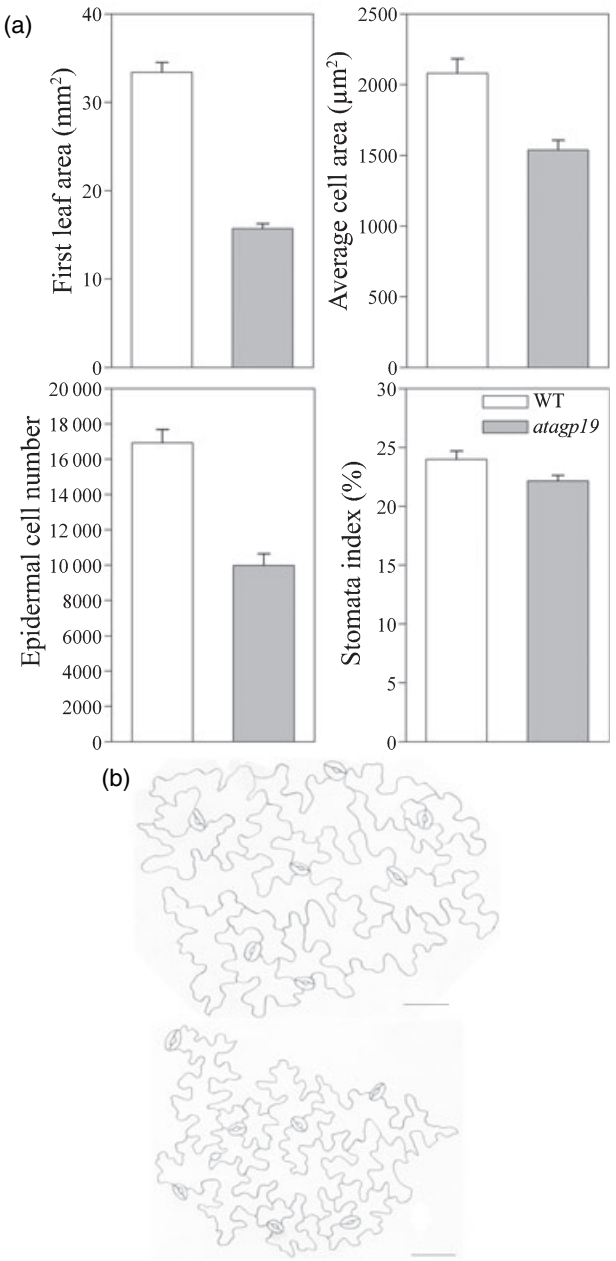

Figure 6. The epidermis of *atagp19* mutant first leaves contained smaller and fewer cells.
(a) Three-week-old first leaves of the *atagp19* mutant were only half the size of those of wild type (WT), consistent with smaller and fewer cells in the *atagp19* abaxial epidermis. However, the *atagp19* mutant and WT had similar stomata to total epidermal cell ratios. Error bars indicate SE ($n = 9$).
(b) Drawing tube images of WT (top) and *atagp19* (bottom) abaxial epidermis. Bars = 50 μm.

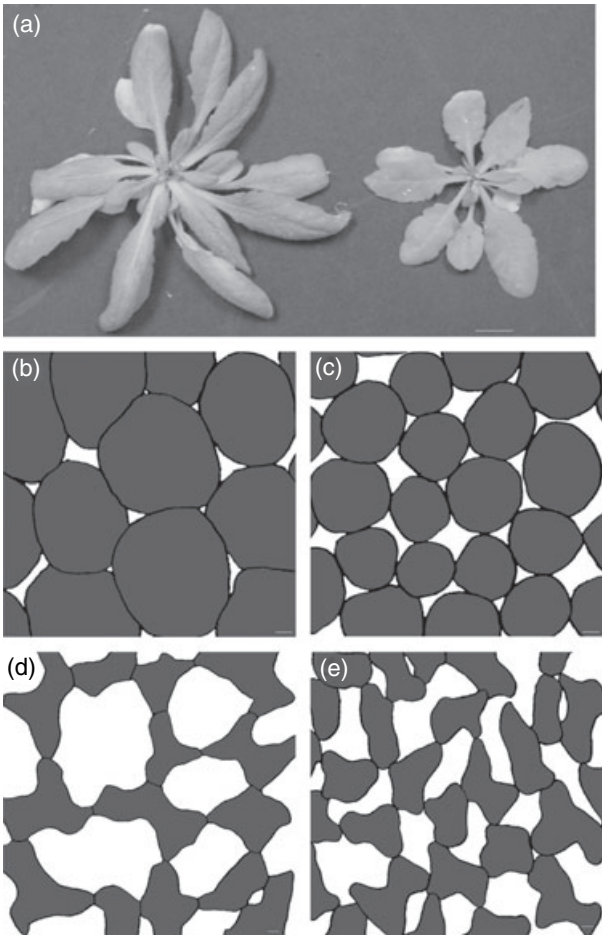

Figure 7. Mature *atagp19* mutant rosette leaves were flat.
(a) 49-day-old rosettes of WT (left) and *atagp19* mutant plants (right). The inflorescence stems were removed from the rosettes before the image was taken.
(b,c) Paradermal views of palisade mesophyll cells in wild type (WT) and the *atagp19* mutant, respectively.
(d,e) Paradermal views of spongy mesophyll cells in WT and the *atagp19* mutant, respectively. Gray represents cells, and white represents intercellular space. At least ten WT and *atagp19* mutant leaves were examined, respectively.
Bars = 1 cm in (a), and 10 μm in (b)–(e).

in shape and more densely packed than in WT (Figure 7d,e); this abnormal cellular packing may result in the flat leaves in the *atagp19* mutant. In contrast, spongy mesophyll cells in WT were irregular in shape and characterized by large intercellular spaces.

Compromised fertility in the atagp19 *mutant*

The *atagp19* mutant had shorter, more slender inflorescence stems with fewer auxillary branches and side bolts (Figure 8a and Table 2). *atagp19* produced fewer flowers than WT (Figure 8b,c). *atagp19* also had fewer and shorter siliques, fewer seeds per silique, and a higher percentage of sterile siliques (Table 2), resulting in less seed production. More than half of the *atagp19* flowers were fertile, and, although they were smaller than WT flowers, they opened normally and had normal arrangements and numbers of floral organs (Figure 8d). Some *atagp19* sterile flowers were open, while others remained closed (Figure 8e). One reason for sterility was the failure of the stamens to elongate

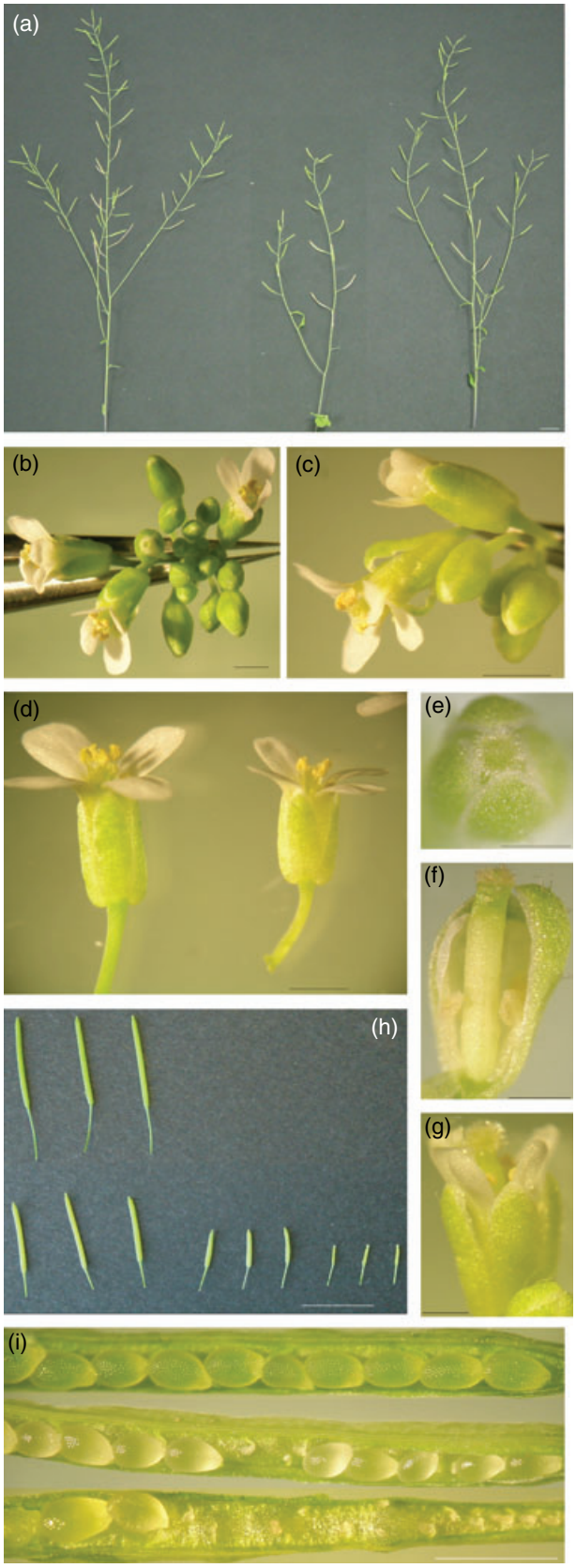

Table 2 Stem and flower comparison between wild type (WT) and *atagp19* mutant plants

Parameters	WT	*atagp19*
Stem length (cm)	33.8 ± 1.1	20.1 ± 1.2
Stem width (mm)	1.2 ± 0.1	0.8 ± 0.1
Silique number	121.0 ± 21.4	19.4 ± 3.2
Silique length (mm)	13.5 ± 0.4	10.8 ± 0.4
Seeds per silique	54.0 ± 2.4	28.2 ± 4.6
Sterile siliques (%)	4.0 ± 0.5	31.5 ± 5.1
Side bolts from shoot apex (>1 cm)	1.3 ± 0.3	0.6 ± 0.3
Auxillary branches	3.1 ± 0.2	2.2 ± 0.2

Values are expressed in mean ± 95% CI ($n > 30$).

beyond the pistil at floral stage 14 (Figure 8f,g), while, in WT, the stamens were longer than the pistil and brushed against the stigma to allow pollination and fertilization (Smyth *et al.*, 1990). Siliques of *atagp19* could be divided into three length ranges, with the longest ones being slightly shorter than WT siliques (Figure 8h). The shortest *atagp19* siliques were completely sterile, while the medium-length siliques were semi-sterile, bearing fewer than five seeds per silique. Even when pollination occurred normally, there was a high percentage of aborted ovules without signs of early seed development (Figure 8i); therefore, shorter stamens did not seem to be the only cause of sterility. Moreover, reciprocal crosses suggested that female reproduction was possibly defective in *atagp19*, because few seeds were recovered when *atagp19* plants were used as female parents, and normal fertility was observed with *atagp19* plants as the male parents (data not shown).

Complementation of the atagp19 *mutant and restoration of WT phenotypes*

As mentioned previously, complementation of the mutant with the WT *AtAGP19* gene under the control of its own

Figure 8. Inflorescence and silique phenotypes of the *atagp19* mutant.
(a) Inflorescence stems of wild-type (WT) (left), *atagp19* mutant (center) and complemented plants (right).
(b,c) Inflorescences of WT and the *atagp19* mutant, respectively.
(d) A WT flower (left) was larger than a fertile *atagp19* mutant flower (right), but the floral organization was similar.
(e) Top view of a closed *atagp19* flower. Sometimes the carpel extended beyond the sepals, as in this case.
(f) A dissected closed *atagp19* flower showing abnormal petal and stamen development.
(g) A sterile *atagp19* flower with the carpel longer than the stamens at floral stage 14, preventing pollination.
(h) Siliques of WT (top) and *atagp19* (bottom) plants. The siliques shown were of representative lengths. The *atagp19* mutant contained an abnormally high proportion of short/sterile siliques (Table 2).
(i) The *atagp19* mutant (center and bottom) had higher aborted ovule rates than the WT (top). The center silique corresponded to longest *atagp19* silique, and bottom silique was of the middle length range in (g).
Bars = 1 cm in (a) and (h), 1 mm in (b)–(d) and (i), and 0.5 mm in (e)–(g).

promoter restored *AtAGP19* mRNA (Figure 4a) as well as the WT phenotypes. In particular, complemented plants displayed normal leaf size, shape, color and growth rate (Figure 5a,b). In addition, stem length and thickness as well as seed production were also restored in the complemented mutants (Figure 8a). These data confirmed that the mutant phenotypes were caused by knockout of *AtAGP19*.

Discussion

AtAGP19 is a lysine-rich, classical AGP *family member*

AtAGP19 is a lysine-rich, classical AGP that is predicted to be anchored to the plasma membrane by a GPI anchor (Borner *et al.*, 2003; Schultz *et al.*, 2002); the GPI anchor prediction is supported by the subcellular localization of AtAGP19 to the plasma membrane (J. Yang and A. Showalter, unpubl. results). This gene is related to two homologous AGP genes in Arabidopsis, *AtAGP17* and *18*, as well as to several other AGP genes characterized to varying extents in several other plant species; all are members of the lysine-rich, classical AGP subfamily. AtAGP19 has relatively low amino acid sequence similarities and identities with AtAGP17 and 18, and is a unique member of the lysine-rich AGP family in Arabidopsis as shown by the phylogeny tree and reflected in its predicted glycosylation pattern (Sun *et al.*, 2005). In addition to arabinogalactan polysaccharide addition sites at non-clustered proline/hydroxyproline residues, AtAGP19 also contains a greater percentage of oligoarabinoside addition sites at clustered proline/hydroxyproline residues compared with its two homologs (Sun *et al.*, 2005).

Expression of lysine-rich AGPs

GUS staining patterns of $P_{AtAGP19}$:GUS transgenic plants are consistent with the Northern blot, microarray and MPSS data. GUS staining is under developmental control and strong in seedlings and young organs. For example, young leaves and young stems show strong GUS activity throughout. As the leaves mature, GUS staining becomes confined to the veins and gradually diminishes. In flowers, the style exhibits intense GUS activity. MPSS analysis further corroborates that *AtAGP19* mRNA levels are high in flowers and developing siliques and low in rosette leaves. Nonetheless, the overall transcription levels of *AtAGP19* are the lowest among the three lysine-rich AGPs.

Expression patterns of *AtAGP18 and AtAGP19* are similar to that of *LeAGP1*, which is strongly expressed in flowers and young stems, moderately expressed in roots and young fruits, and weakly expressed in leaves and old stems (Li and Showalter, 1996). LeAGP1 and PtaAGP6 are both immunolocalized to differentiating stem xylem elements and functionally associated with secondary cell wall thickening and xylem development (Gao and Showalter, 2000; Zhang *et al.*, 2003). Similarly, *AtAGP19* promoter activity is tightly associated with the vascular tissues and is localized to differentiating, but not developed, xylem elements (J. Yang and A. Showalter, unpubl. results). LeAGP1 is also abundant in stylar transmitting tissues, with putative roles in guiding and nourishing pollen tube growth. In contrast, the *CsAGP1* transcript is found throughout cucumber seedlings and may be involved in stem elongation (Park *et al.*, 2003). These proposed functions of other lysine-rich AGPs, which are based largely on expression patterns, have provided guidance in elucidating the roles of AtAGP19 and in studying the *atagp19* mutant.

AtAGP19 functions in plant growth and development, including cell division and expansion

The *atagp19* mutant displays multiple and dramatic mutant phenotypes that are statistically different from WT. These phenotypes occur during both vegetative and reproductive growth, and include altered leaf shape and size, lighter color, slower growth, shorter hypocotyls and inflorescence stems, and compromised fertility. Phenotypes of the *atagp19* mutant correspond to the position and timing of *AtAGP19* expression and indicate that AtAGP19 is essential for normal plant growth and development, including leaf development, stem elongation and seed production. It is not yet clear how loss of AtAGP19 results in lower pigment levels and a slower growth rate in *atagp19*. With respect to reproduction, it is likely that the high percentage of aborted ovules seen in *atagp19* siliques are a result of several factors, such as abnormal stamen development, compromised female gametogenesis, and poor pollen tube guidance in the style.

AtAGP19 function is regulated by light with respect to seedling growth. In light, *atagp19* mutant hypocotyls are approximately 75% as long as WT, but there is no length difference when grown in the dark. *AtAGP19* expression, as determined by GUS staining, is found in both light- and dark-grown Arabidopsis seedlings. Similarly, *LeAGP1* transcription is not affected by light (Li and Showalter, 1996). Thus, this light-regulated function of AtAGP19 occurs at a post-transcriptional level and probably involves interactions with other components that are more directly regulated by light to control hypocotyl length.

Plant growth involves cell division and cell elongation. The *atagp19* mutant has fewer abaxial epidermal cells in rosette leaves, indicating a decrease in cell division. Histological analyses further indicate a reduction in cell division in stems (J. Yang and A. Showalter, unpubl. results). AtAGP19 also plays a role in cell expansion; this is seen from the shorter hypocotyl cells, smaller rosette epidermal cells and more regularly shaped spongy mesophyll cells in the *atagp19* mutant. Therefore, the dwarf phenotype of *atagp19* is a result of impaired cell division and cell expansion. Previous work has indicated that AGPs, either individually or

collectively, function in cell division and expansion (Langan and Nothnagel, 1997; Lee *et al.*, 2005; Majewska-Sawka and Nothnagel, 2000; Park *et al.*, 2003; Serpe and Nothnagel, 1994; Shi *et al.*, 2003; Willats and Knox, 1996), and the findings reported here support these functional roles.

The precise mechanism(s) for the observed function of AtAGP19 in plant growth and development, including cell division and expansion, remains to be elucidated. There are several indications, however, that AtAGP19 acts through cellular signaling pathways. First, the *atagp19* mutant has multiple abnormal phenotypes, and the disruption of one or more signaling pathways in this mutant would provide a plausible explanation to account for these pleiotropic effects. Second, many of the phenotypes observed are related to alterations of phytohormone pathways. Third, AtAGP19 has a predicted GPI anchor, and GPI-anchored proteins play putative roles in cellular signaling and communication (Schultz *et al.*, 1998; Youl *et al.*, 1998).

Functional relationships of AtAGP17, 18 *and* 19

Despite some changes in *AtAGP17* and *18* mRNA accumulation in the *atagp19* mutant and the similar expression patterns of *AtAGP18* and *19*, there appears to be little functional compensation. This idea is further supported by the observation that no additional mutant phenotypes are seen in *atagp17 atagp19* and *atagp18 atagp19* double mutants produced by crossing the SALK_101062 and SALK_117268 lines with *atagp19*, respectively (J. Yang and A. Showalter, unpubl. results). In *AtAGP17* or *AtAGP18* T-DNA insertion mutants and *AtAGP18* RNAi mutants, no gene compensation by the other lysine-rich AGPs occurs in the organs examined (Acosta-Garcia and Vielle-Calzada, 2004; J. Yang and A. Showalter, unpubl. results). Overall, the picture that emerges from the above expression data and from characterization of mutants of the three lysine-rich AGPs is that all three lysine-rich AGPs have unique and independent functions in Arabidopsis. Future experiments to test this idea might involve determining whether the other two lysine-rich AGP genes can complement a specific lysine-rich AGP mutant (e.g. *atagp19*) when expressed under the control of the promoter of the mutated AGP gene (e.g. $P_{AtAGP19}$:*AtAGP17* and $P_{AtAGP19}$:*AtAGP18*).

AGP mutants provide insight into AGP function

AGP mutants are helping to identify the function of AGPs and provide a framework to explore the underlying mechanisms responsible for AGP function. A study of the overexpression of LeAGP1 connected this AGP to cytokinin signaling (Sun *et al.*, 2004a). In contrast, the *atagp19* mutant responds to cytokinin in a way similar to that in WT; for example, chlorophyll content, primary root length and lateral root numbers of both WT and mutant seedlings decrease in response to cytokinin 6-benzyl-amino-purine concentrations higher than 0.005 μM. These observations imply that the function of AtAGP19 may be different from that of LeAGP1 (J. Yang and A. Showalter, unpubl. results). Analysis of a null mutant of *AtAGP30*, a non-classical AGP gene, suggests that it plays a role in ABA responses and root regeneration (van Hengel and Roberts, 2003). The implication of AGPs in phytohormone pathways is in line with our hypothesis that AtAGP19 is involved in cell signaling pathways. Considering the other two lysine-rich AGPs in Arabidopsis, an insertion in the promoter region of *AtAGP17* results in reduced binding to *Agrobacterium* (Gaspar *et al.*, 2004; Nam *et al.*, 1999), while *AtAGP18* RNAi mutants display high ovule abortion rates (Acosta-Garcia and Vielle-Calzada, 2004). Similar to the *AtAGP18* RNAi mutants, *atagp19* mutant siliques contain many aborted ovules; the reason for this remains unknown. On the other hand, roots of the *atagp19* mutant have normal *Agrobacterium*-binding capacities (J. Yang and A. Showalter, unpublished results).

The defects in cell expansion in the *atagp19* mutants are reminiscent of those in three other AGP mutants. Moss AGP1 RNAi plants represent one such mutant and display reduced apical cell extension (Lee *et al.*, 2005). A mutant of *AtFLA4* in Arabidopsis shows abnormal cell expansion (Shi *et al.*, 2003), while tobacco plants over-expressing CsAGP1 are taller due to greater stem elongation (Park *et al.*, 2003). Together with this study, there is now compelling evidence that AGPs are required for normal cell expansion. In addition, a double xylogen mutant in Arabidopsis (*atxyp1 atxyp2*) has shown discontinuous leaf venation patterns (Motose *et al.*, 2004). Although this particular phenotype is not observed in the *atagp19* mutant, *atagp19* has smaller vascular cylinders in the mature roots compared to WT. The smaller vascular region in the mutant is due to fewer cells and not to changes in cell size, shape and wall thickness of the xylem elements, which appear normal (J. Yang and A. Showalter, unpubl. results). Considering all AGP mutants examined to date, the *atagp19* mutant shows the broadest and most readily apparent phenotypes without the need to resort to special screens. The underlying mechanisms explaining how AtAGP19, as well as the other AGPs from characterized mutants, regulate various cellular and physiological processes remain to be elucidated, but efforts are underway to address this important and challenging issue.

Experimental procedures

Bioinformatics

The similarities/identities of lysine-rich AGPs were obtained with MatGAT (matrix global alignment tool), version 2.01, using the BLOSUM62 algorithm (http://www.angelfire.com/nj2/arabidopsis/MatGAT.html) (Campanella *et al.*, 2003).

Microarray data for gene expression in WT Arabidopsis under normal conditions were obtained from https://http://www.geneves-

tigator.ethz.ch/(Zimmermann *et al.*, 2004). Microarray data for gene expression under stresses were retrieved from TAIR Microarray Expression Search (http://www.arabidopsis.org/servlets/Search?action=new_search&type=expression) and analyzed. Signature MPSS data were from http://mpss.udel.edu/at/ (Meyers *et al.*, 2004), and transcript per million values for 17 bp and 21 bp signatures were averaged and then plotted.

Plant material and growth conditions

WT and *atagp19* Arabidopsis plants were Columbia-0 ecotype. Plants were grown under 16 h light/8 h dark conditions in soil or on MS plates consisting of 1 × MS (Murashige and Skoog) medium, 1% sucrose and 0.8% agar.

Mutant verification and sequencing

In order to isolate and verify the *atagp19* mutant, two *AtAGP19*-specific primers (5′-CAACAAGATGCATCAAGTCTTACC-3′ and 5′-GTGCTGGTGGTGGTGATACAG-3′), and one T-DNA-specific primer (5′-TGGTTCACGTAGTGGGCCATCG) were designed using the SIGnAL T-DNA verification primer design tool (http://signal.salk.edu/cgi-bin/tdnaexpress). Sequencing reactions were performed using a BigDye Terminator version 3.1 cycle sequencing kit (Applied Biosystems, http://www.appliedbiosystems.com) according to the manufacturer's instructions, and run on an ABI 310 genetic analyzer (Applied Biosystems).

RNA extraction, Northern blotting and RT-PCR

Total RNA was extracted using the RNeasy plant mini kit (Qiagen Inc., http://www.qiagen.com), and on-column DNase digestion was conducted for RT-PCR purposes. Northern blotting was carried out according to the method described by Sun *et al.* (2005). RT-PCR was performed using a OneStep RT-PCR Kit (Qiagen Inc.) using *AtAGP19* mRNA-specific primers 5′-CTGCTCTCATCTCTTCCTTTAGTG-3′ and 5′-ATTGAGCCACATTACTGCTCTTCC-3′.

Transformation

Agrobacterium strain LBA4404 was transformed by electroporation using the GENE PULSER II system (Bio-Rad, http://www.bio-rad.com) according to the manufacturer's instructions. Arabidopsis plants were transformed by the floral dip method (Clough and Bent, 1998).

GUS staining

For the $P_{AtAGP19}$**:GUS** construct, the 1.8 kb *AtAGP19* promoter sequence was amplified using the primer combination 5′-CCGGTTAATTAATGAAACTGCCTAGTCGGAACCTGA-3′ and 5′-AAATGGCGCGCCTGTGTTGTGGAGGAAGCTACAAGA-3′, and inserted into *Pac*I and *Asc*I sites of the binary vector pMDC164 (Curtis and Grossniklaus, 2003). The same promoter sequence was also used for the complementation experiment described below; this complementation experiment indicated that this promoter successfully drove *AtAGP19* expression.

At least one plant from each of the 15 independent transgenic lines harboring the $P_{AtAGP19}$**:GUS** fusion was tested, and representative GUS staining patterns are presented. Samples were incubated in a GUS staining solution (0.5 M sodium phosphate, 0.2 mM potassium ferricynide, 0.2 mM potassium ferrocynide, 0.5% Triton X-100 and 2 mM X-GlcA, pH 7.2) at 37°C for 12–24 h. After staining, samples were cleared in absolute ethanol, and images were taken under the ACE light source (Schott-Fostec L.L.C., Auburn, NY, USA) using a Nikon COOLPIX 5400 digital camera connected to a Nikon binocular stereo dissecting microscope SMZ1500 (Nikon, http://www.nikonusa.com).

Phenotypic analyses

Chlorophyll levels in 14-day-old WT and *atagp19* plants and anthocyanin content in 24-day-old WT and *atagp19* plants were assayed according to published methods (Arnon, 1949; Laby *et al.*, 2000).

Reproduction was examined in mature WT and *atagp19* plants immediately after they finished flowering. Stem height was measured with a ruler, and stem width was measured using IMAGE-PRO software (Media Cybernetics Inc., http://www.mediacy.com). Flowers and fully expanded siliques from same positions on WT and *atagp19* plants were compared, and the siliques close to either end of inflorescence stems were avoided.

In order to study leaf cells, fully elongated first leaves (21-day-old plants grown in soil) were cleared in methanol and then in lactic acid. Leaf abaxial epidermal cells and mesophyll cells were drawn using a DIC microscope equipped with a drawing tube. Analyses of epidermal cells were carried out according to the methods described by Autran *et al.* (2002).

After 7-day-old seedlings grown on horizontal plates were cleared as described above, digital pictures of hypocotyls were taken. Hypocotyls and hypocotyl epidermal cells were analyzed with IMAGE J software (http://rsb.info.nih.gov/ji/).

Statistics

Statistical analyses and data plotting and were performed using SIGMA PLOT 8.0 (SPSS Inc., http://www.spss.com).

Complementation of the atagp19 *mutant*

The WT *AtAGP19* gene sequence, including its endogenous promoter and coding sequence (from the nucleotide at position 1836 upstream of the *AtAGP19* start codon to the stop codon), was amplified using primers 5′-CCGGTTAATTAATGAAACTGCCTAGTCGGAACCTGA-3′ and 5′-CCCGCGAGCTCTTAGGCTGTCATAGCAAGTAGAAAG-3′, and cloned into the binary vector pMDC110 between the *Pac*I and *Sac*I sites (Curtis and Grossniklaus, 2003), followed by the nos terminator.

Acknowledgements

This work was supported by a grant from the National Science Foundation (IBN-0110413) and by a Baker Fund Award from Ohio University. T-DNA mutant lines of *AtAGP17*, *18* and *19* were obtained from the SALK Institute and ABRC. The authors would like to thank Dr Ming Chen, Dr Wenxian Sun and Dr Sarah Wyatt for suggestions and advice, and Dr Ahmed Faik for critical reading of the manuscript.

References

Acosta-García, G. and Vielle-Calzada, J.-P. (2004) A classical arabinogalactan protein is essential for the initiation of female gametogenesis in Arabidopsis. *Plant Cell*, **16**, 2614–2628.

Alonso, J.M., Stepanova, A.N., Leisse, T.J. *et al.* (2003) Genome-wide insertional mutagenesis of *Arabidopsis thaliana*. *Science*, **301**, 653–657.

Arnon, D.I. (1949) Copper enzymes in isolated chloroplasts. Polyphenoloxidase in *Beta vulgaris*. *Plant Physiol.* **24**, 1–15.

Autran, D., Jonak, C., Belcram, K., Beemster, G.T.S., Kronenberger, J., Grandjean, O., Inzé, D. and Traas, J. (2002) Cell numbers and leaf development in *Arabidopsis*: a functional analysis of the STRUWWELPETER gene. *EMBO J.* **21**, 6036–6049.

Borner, G.H.H., Lilley, K.S., Stevens, T.J. and Dupree, P. (2003) Identification of glycosylphosphatidylinositol-anchored proteins in Arabidopsis. A proteomic and genomic analysis. *Plant Physiol.* **132**, 568–577.

Campanella, J.J., Bitincka, L. and Smalley, J. (2003) MatGAT: an application that generates similarity/identity matrices using protein or DNA sequences. *BMC Bioinformatics*, **4**, 29.

Clough, S.J. and Bent, A.F. (1998) Floral dip: a simplified method for *Agrobacterium*-mediated transformation of *Arabidopsis thaliana*. *Plant J.* **16**, 735–743.

Curtis, M.D. and Grossniklaus, U. (2003) A gateway cloning vector set for high-throughput functional analysis of genes in planta. *Plant Physiol.* **133**, 462–469.

Gao, M. and Showalter, A.M. (1999) Yariv reagent treatment induces programmed cell death in *Arabidopsis* cell cultures and implicates arabinogalactan protein involvement. *Plant J.* **19**, 321–331.

Gao, M. and Showalter, A.M. (2000) Immunolocalization of LeAGP-1, a modular arabinogalactan-protein, reveals its developmentally regulated expression in tomato. *Planta*, **210**, 865–874.

Gao, M., Kieliszewski, M.J., Lamport, D.T.A. and Showalter, A.M. (1999) Isolation, characterization and immunolocalization of a novel, modular tomato arabinogalactan-protein corresponding to the LeAGP-1 gene. *Plant J.* **18**, 43–55.

Gaspar, Y.M., Johnson, K.L., McKenna, J.A., Bacic, A. and Schultz, C.J. (2001) The complex structures of arabinogalactan-proteins and the journey towards understanding function. *Plant Mol. Biol.* **47**, 161–176.

Gaspar, Y.M., Nam, J., Schultz, C.J., Lee, L.-Y., Gilson, P.R., Gelvin, S.B. and Bacic, A. (2004) Characterization of the Arabidopsis lysine-rich arabinogalactan-protein *AtAGP17* mutant (*rat1*) that results in a decreased efficiency of Agrobacterium transformation. *Plant Physiol.* **135**, 2162–2171.

Gilson, P.R., Gaspar, Y.M., Oxley, D., Youl, J.J. and Bacic, A. (2001) NaAGP4 is an arabinogalactan protein whose expression is suppressed by wounding and fungal infection in *Nicotiana alata*. *Protoplasma*, **215**, 128–139.

van Hengel, A.J. and Roberts, K. (2003) AtAGP30, an arabinogalactan-protein in the cell walls of the primary root, plays a role in root regeneration and seed germination. *Plant J.* **36**, 256–270.

van Hengel, A.J., van Kammen, A. and de Vries, S.C. (2002) A relationship between seed development, arabinogalactan-proteins (AGPs) and the AGP mediated promotion of somatic embryogenesis. *Physiol. Plant.* **114**, 637–644.

Kieliszewski, M.J. and Shpak, E. (2000) Synthetic genes for the elucidation of glycosylation codes for arabinogalactan-proteins and other hydroxyproline-rich glycoproteins. *Cell. Mol. Life Sci.* **58**, 1386–1398.

Laby, R.J., Kincaid, M.S., Kim, D. and Gibson, S.I. (2000) The *Arabidopsis* sugar-insensitive mutants *sis4* and *sis5* are defective in abscisic acid synthesis and response. *Plant J.* **23**, 587–596.

Langan, K.J. and Nothnagel, E.A. (1997) Cell surface arabinogalactan-proteins and their relation to cell proliferation and viability. *Protoplasma*, **196**, 87–98.

Lee, K.J.D., Sakata, Y., Mau, S.-L., Pettolino, F., Bacic, A., Quatrano, R.S., Knight, C.D. and Knox, J.P. (2005) Arabinogalactan proteins are required for apical cell extension in the moss Physcomitrella patens. *Plant Cell*, **17**, 3051–3065.

Li, S. and Showalter, A.M. (1996) Cloning and developmental/stress-regulated expression of a gene encoding a tomato arabinogalactan protein. *Plant Mol. Biol.* **32**, 641–652.

Majewska-Sawka, A. and Nothnagel, E.A. (2000) The multiple roles of arabinogalactan proteins in plant development. *Plant Physiol.* **122**, 3–10.

Mashiguchi, K., Yamaguchi, I. and Suzuki, Y. (2004) Isolation and identification of glycosylphosphatidylinositol-anchored arabinogalactan proteins and novel β-glucosyl Yariv-reactive proteins from seeds of rice (*Oryza sativa*). *Plant Cell Physiol.* **45**, 1817–1829.

Meyers, B.C., Lee, D.K., Vu, T.H., Tej, S.S., Edberg, S.B., Matvienko, M. and Tindell, L.D. (2004) Arabidopsis MPSS. An online resource for quantitative expression analysis. *Plant Physiol.* **135**, 801–813.

Motose, H., Sugiyama, M. and Fukuda, H. (2001) An arabinogalactan protein(s) is a key component of a fraction that mediates local intercellular communication involved in tracheary element differentiation of Zinnia mesophyll cells. *Plant Cell Physiol.* **42**, 129–137.

Motose, H., Sugiyama, M. and Fukuda, H. (2004) A proteoglycan mediates inductive interaction during plant vascular development. *Nature*, **429**, 873–878.

Nam, J., Mysore, K.S., Zheng, C., Knue, M.K. and Gelvin, S.B. (1999) Identification of T-DNA tagged *Arabidopsis* mutants that are resistant to transformation by *Agrobacterium*. *Mol. Gen. Genet.* **261**, 429–438.

Park, M.H., Suzuki, Y., Chono, M., Knox, J.P. and Yamaguchi, I. (2003) *CsAGP1*, a gibberellin-responsive gene from cucumber hypocotyls, encodes a classical arabinogalactan protein and is involved in stem elongation. *Plant Physiol.* **131**, 1450–1459.

Schultz, C.J., Gilson, P.R., Oxley, D., Youl, J.J. and Bacic, A. (1998) GPI-anchors on arabinogalactan-proteins: implications for signalling in plants. *Trends Plant Sci.* **3**, 426–431.

Schultz, C.J., Rumsewicz, M.P., Johnson, K.L., Jones, B.J., Gaspar, Y.M. and Bacic, A. (2002) Using genomic resources to guide research directions. The arabinogalactan protein gene family as a test case. *Plant Physiol.* **129**, 1448–1463.

Serpe, M.D. and Nothnagel, E.A. (1994) Effects of Yariv phenylglycosides on Rosa cell suspension: evidence for the involvement of arabinogalactan-proteins in cell proliferation. *Planta*, **193**, 542–550.

Shi, H., Kim, Y., Guo, Y., Stevenson, B. and Zhu, J.-K. (2003) The Arabidopsis *SOS5* locus encodes a putative cell surface adhesion protein and is required for normal cell expansion. *Plant Cell*, **15**, 19–32.

Showalter, A.M. (2001) Arabinogalactan-proteins: structure, expression and function. *Cell. Mol. Life Sci.* **58**, 1399–1417.

Smyth, D.R., Bowman, J.L. and Meyerowitz, E.M. (1990) Early flower development in *Arabidopsis*. *Plant Cell*, **2**, 755–767.

Sun, W., Kieliszewski, M.J. and Showalter, A.M. (2004a) Overexpression of tomato LeAGP-1 arabinogalactan-protein promotes lateral branching and hampers reproduction development. *Plant J.* **40**, 870–881.

Sun, W., Zhao, Z., Hare, M.C., Kieliszewski, M.J. and Showalter, A.M. (2004b) Tomato LeAGP-1 is a plasma membrane-bound, glycosylphosphatidylinositol-anchored arabinogalactan-protein. *Physiol. Plant.* **120**, 319–327.

Sun, W., Xu, J., Yang, J., Kieliszewski, M.J. and Showalter, A.M. (2005) The lysine-rich arabinogalactan-protein subfamily in *Arabidopsis*: gene expression, glycoprotein purification and biochemical characterization. *Plant Cell Physiol.* **46**, 975–984.

Suzuki, Y., Kitagawa, M., Knox, J.P. and Yamaguchi, I. (2002) A role for arabinogalactan proteins in gibberellin-induced α-amylase production in barley aleurone cells. *Plant J.* **29**, 733–741.

Willats, W.G.T. and Knox, J.P. (1996) A role for arabinogalactan-proteins in plant cell expansion: evidence for studies on the interaction of β-glucosyl Yariv reagent with seedlings of *Arabidopsis thaliana*. *Plant J.* **9**, 919–925.

Wu, H., Wong, E., Ogdahi, J. and Cheung, A.Y. (2000) A pollen tube growth-promoting arabinogalactan protein from *Nicotiana alata* is similar to the tobacco TTS protein. *Plant J.* **22**, 165–176.

Yariv, J., Rapport, M.M. and Graf, L. (1962) The interaction of glycosides and saccharides with antibody to the corresponding phenolazo glycoside. *Biochem. J.* **85**, 383–388.

Yariv, J., Lis, H. and Katchalski, E. (1967) Precipitation of arabic acid and some seed polysaccharides by glycosylphenylazo dyes. *Biochem. J.* **105**, 1c–2c.

Youl, J.J., Bacic, A. and Oxley, D. (1998) Arabinogalactan-proteins from *Nicotiana alata* and *Pyrus communis* contain glycosylphosphatidylinositol membrane anchors. *Proc. Natl Acad. Sci. USA*, **95**, 7921–7926.

Zhang, Y., Brown, G., Whetten, R., Loopstra, C.A., Neale, D., Kieliszewski, M.J. and Sederoff, R.R. (2003) An arabinogalactan protein associated with secondary cell wall formation in differentiating xylem of loblolly pine. *Plant Mol. Biol.* **52**, 91–102.

Zhao, Z., Tan, L., Showalter, A.M., Lamport, D.T.A. and Kieliszewski, M.J. (2002) Tomato LeAGP-1 arabinogalactan-protein purified from transgenic tobacco corrobates the Hyp contiguity hypothesis. *Plant J.* **31**, 431–444.

Zimmermann, P., Hirsch-Hoffmann, M., Hennig, L. and Gruissem, W. (2004) GENEVESTIGATOR. Arabidopsis microarray database and analysis toolbox. *Plant Physiol.* **136**, 2621–2632.

